

Research article

Biopolymer Geogrids for Geotechnics

Gabriel Oliveira*, and Isabel Falorca

University of Beira Interior, Centre of Materials and Building Technologies (C•MADE-UBI), Faculty of Engineering, Calçada Fonte do Lameiro, 6200-358 Covilhã, Portugal

Abstract.

This study focused on the mechanical characterisation of 3D printed biopolymer geogrids for civil and geotechnical engineering applications. The polylactic acid specimens were designed based on first-order similitude conditions and were produced by fused deposition modelling techniques. An experimental programme was carried out to investigate the mechanical behaviour of 1:2 scale model geogrids undergoing tensile loading conditions, in order to explore their use in soil reinforcement and stabilisation of geomaterials. The secant stiffness at 2.0% of strain and the ultimate tensile strength were used for this purpose. The results showed an average tensile strength of 4.5 ± 0.5 kN/m, which is in good agreement with that of fossil oil-derived polymer prototypes, while presenting a significantly lower elongation at failure. The printing process appeared stable and replicable. The influence of degradation on the tensile properties of 3D printed polylactic acid geogrids over time still needs to be studied.

Corresponding Author: Gabriel Oliveira; email: gabriel.marchi.oliveira@ubi.pt

Published 10 August 2022

Publishing services provided by Knowledge E

© Gabriel Oliveira, and Isabel Falorca. This article is distributed under the terms of the [Creative Commons Attribution License](#), which permits unrestricted use and redistribution provided that the original author and source are credited.

Selection and Peer-review under the responsibility of the FibEnTech21 Conference Committee.

Keywords: geogrid, additive manufacturing, biopolymer, tensile strength, geotechnics

1. Introduction

A geogrid is a planar mesh structure that can be used to reinforce and stabilise soil [1] and has apertures into which soil particles can be locked, in order to make construction more efficient. Figure 1 illustrates the component elements of a geogrid, where ribs and junctions are the tensile load-bearing parts that interact with the environment in which they are inserted. According to [2] when the load-bearing parts have high tensile strength in only one direction, the geogrid is considered uniaxial and biaxial when it has high tensile strength in the two main directions. Triaxial geogrids exhibit high tensile strength in multi-directions of the geogrid plane. So, the most significant characteristics include the suitable aperture size to interact with the surrounding soil particles and the sufficient tensile strength in the short- and long-term. Over the last four decades, much geogrid types have been developed, using a variety of different technologies, considering environmental and economic factors. Geogrids can be manufactured by stitch bonding fabrics made of polymer filaments followed by coating, or by knitting, or

OPEN ACCESS

by welding oriented polymer strips. They can also be formed by extruding a polymer sheet material that is provided with a defined pattern of holes and then stretched in a controlled orientation [3]. Most geogrids are produced from fossil oil-derived polymers. To offset the negative impact of using synthetic materials, biopolymer geogrids are increasingly being explored for civil and geotechnical engineering applications. Among the natural-derived and renewable biopolymers, the polylactic acid (PLA) can ensure several advantages in terms of sustainability and eco-compatibility [4].

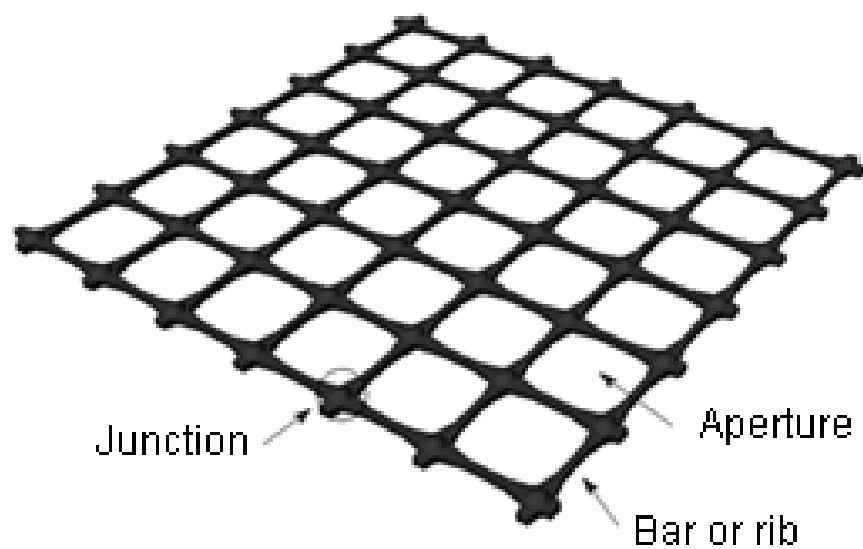


Figure 1: Extruded biaxial geogrid made up of ribs and junction knobs.

A common practice in geotechnical research studies is to use physical modelling techniques in order to infer the prototype behaviour. Therefore, the properties of geogrids (e.g., geometry and tensile strength) must be properly scaled [5] when preparing a small-scale version of geogrids. Recently, model geogrids were successfully produced by a 3D printing process [6]. The 3D printing is an additive manufacturing process to make objects from digital models through the successive layer-by-layer deposition of digital materials. Among several 3D printing methods, fused deposition modelling (FDM) is the most used. Typically, the polymer materials are melted and extruded in the form of filaments and then deposited over the bed where the parts are built, solidifying, and integrating with the surrounding filaments until the product is finished. There are many parameter settings that can be selected for the FDM process, which will affect the mechanical properties of the final product [7]. Hence, mechanical properties of the printed materials are important measures of product quality, thus relying strongly on experiments.

In this study, the procedure to prepare model geogrids with properly scaled tensile behaviour for small-scale laboratory tests are presented. Further, the 3D printed specimens made of PLA and the proposed testing programme are described. The main objective was to evaluate the tensile properties of model geogrids such as the secant stiffness and the ultimate tensile strength in order to explore its use in soil reinforcement and stabilisation of geomaterials.

2. Material and methods

Specimens were designed by scaling down the dimensions of commercially available biaxial geogrids, so that they could be used to investigate the mechanical behaviour of layered geomaterials in the follow-up experimental study [8]. The tensile strength of the model geogrid was $1/N^2$ times of that of the prototype (where N is the scale factor), assuming identical material characteristics and identical geogrid strains in model and prototype. Table 1 presents the geometric characteristics of the model geogrids that were derived using a scale factor of 2. Using PLA white filament, the biaxial geogrids were produced by a high precision open-source FDM printer (Fig.2). Table 2 shows the 3D printing parameters considered in this study. The printing plane was XY, and the layers were summed along the Z direction. Therefore, the printing was in X direction with a raster angle orientation sequence of $\pm 45^\circ$ in order to have a criss-cross sequence with rectilinear infill. The nominal specimen dimensions were 100 mm in width and 100 mm in length, considering the recommendations of NP EN ISO 10319 [9] for the preparation of test specimens. To ensure the repeatability of the results, two specimens were printed and one of them was cut into longitudinal rib pieces with 100 mm length.

TABLE 1: Summary of characteristics of model geogrids.

Parameter	Value
Grid opening size (mm)	17.9
Rib width (mm)	1.55
Rib thickness (mm)	1.20
Rib cross sectional area, (mm ²)	1.86
Percentage of open area (%)	80.2
Junction thickness (mm)	2.0

The uniaxial tensile tests were carried out at a controlled strain rate, in a universal testing machine at the Department of Textile Science and Technology of the University of Beira Interior as shown in Fig.3. Since a standardised tensile test method for FDM printed geogrids has not yet been developed, the procedure specified in NP EN ISO

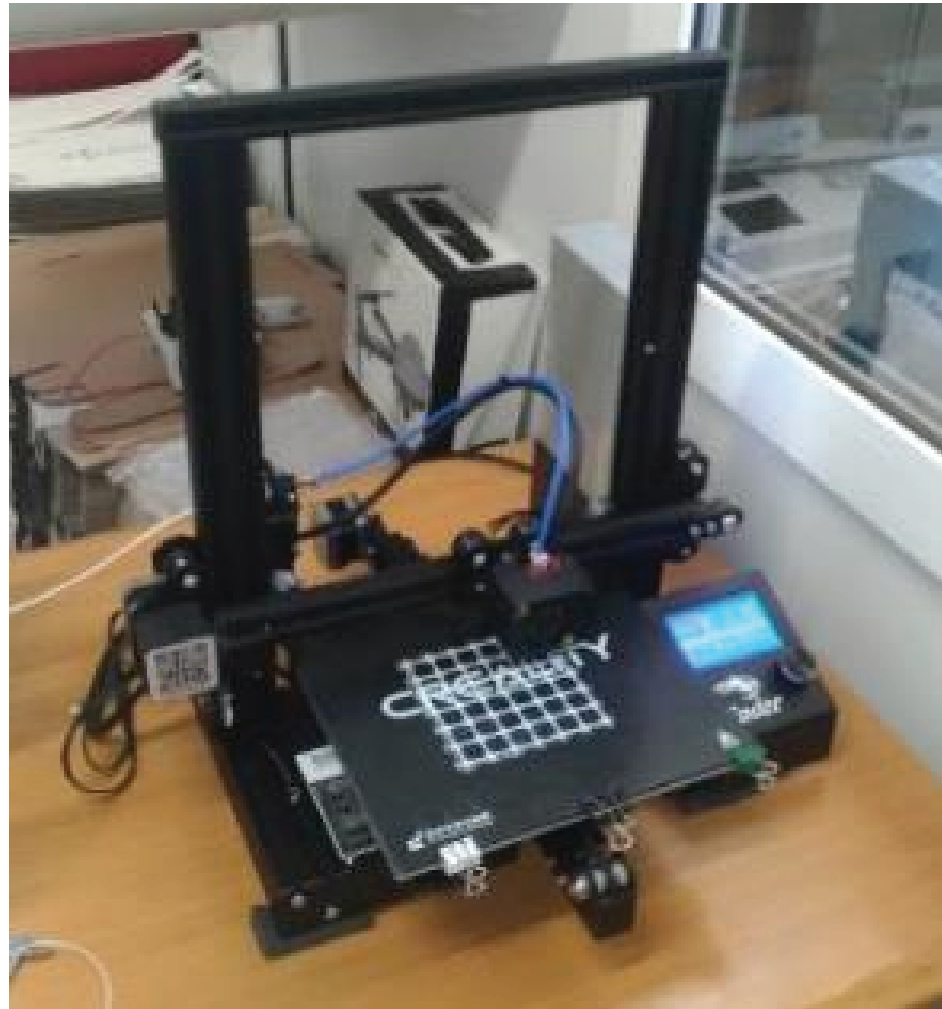


Figure 2: 3D printer used in this study.

TABLE 2: FDM process parameters during 3D printing of specimens.

Parameter	Value	Parameter	Value
Nozzle diameter (mm)	0.4	Printing speed (mm/s)	55
Extrusion temperature (°C)	220	Layer thickness (mm)	0.1
Infill density (%)	100	Raster width (mm)	0.5
Raster angle (°)	45	Fill pattern	rectilinear
Number of perimeters	1	Bed temperature (°C)	N/A

10319 [9] for geosynthetics testing was used, considering the details described below. The distance between the jaws at the start of the test was adjusted to give an effective length of 50 ± 1 mm and then both ends of the specimen were clamped in order to prevent both the specimen damage and the slippage during the progress of the test. The load cell was attached to the movable compressive block jaw in a rigid and perpendicular position, and its force range was selected such that the specimen failure occurs between 30% and 90% of full-scale force. The specimens were stretched at a

constant strain rate of 1.0 mm/min, at room temperature of 20 °C and 50% RH, until a sudden drop associated with the failure of the specimen was recorded. In this study, experiments were conducted on two test specimens, as summarised in Table 3.



Figure 3: Experimental setup during tensile testing of the model geogrid.

TABLE 3: Details of the tensile testing program.

Test specimen	Geogrid	Longitudinal geogrid rib
Test code	grid#18	rib#18
Number of tensile elements within the test specimen	5	1
Load cell capacity (N)	1000	200

The data obtained from the tests were analysed to calculate the tensile strength, strain at maximum load, and the secant stiffness of the test specimens. The tensile force was calculated directly from the recorded maximum load, and the secant stiffness at a specified strain was calculated by applying the Equation 1, where F is the load determined at the specified strain ϵ , N_m is the minimum number of tensile elements

within a one metre width of geogrid, and N_s is the number of tensile elements within the test specimen.

$$J_{sec} = \frac{F \times N_m}{\varepsilon \times N_s} (1)$$

3. Results and discussion

The test results were represented as tensile strength-strain relationships that showed the usual behaviour of polymer materials with brittle failure. Figure 4 shows the engineering tensile curves of the 3D printed PLA specimens. As can be observed, the behaviour is characterised by a noticeable elastic deformation stage, where the tensile strength is proportional to the strain up to a strain of about 2%. It was verified that engineering tensile curves were similar to each other, indicating that tensile properties would not be changed using different test specimens. Such results demonstrate the repeatability of the results. Grid specimens exhibited a very variable behaviour after the peak strength, due to the progressive failure of the longitudinal ribs.

The tensile properties that arise from the analysis of the results are summarised in Table 4. In terms of ultimate tensile strength, model geogrids were characterised by an average tensile strength of 4.5 ± 0.5 kN/m. Similar results were reported by [4].

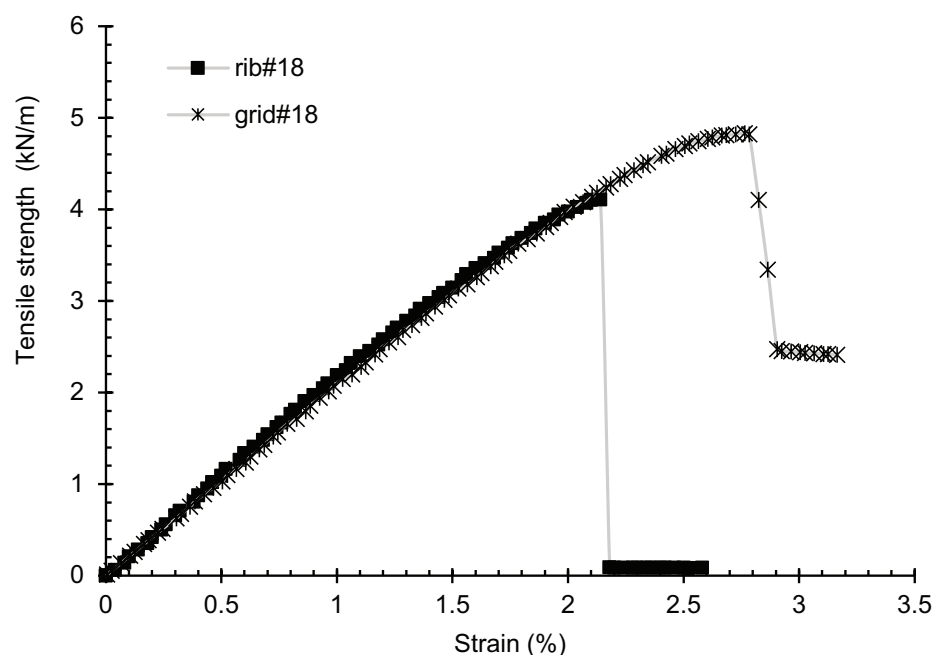


Figure 4: Tensile strength-strain curves of grid and rib PLA specimens.

TABLE 4: Mechanical properties of 3D printed PLA model geogrids.

Properties	grid#18	rib#18
Elongation at ultimate tensile strength (%)	2.8	2.1
Ultimate tensile strength (kN/m)	4.8	4.1
Secant stiffness at 2.0% strain (kN/m)	199.0	198.7

Table 5 presents the parameter values to be considered with the downscaling of the prototype geogrids with a scale factor of 2 ($N = 2$) under 1-g conditions for geogrids with 18 mm aperture size.

TABLE 5: Parameters of prototype geogrid with 36 mm aperture size at 1-g and $N = 2$.

Parameters	PLA geogrid prototype
Elongation at ultimate tensile strength, ϵ_r (%)	2.8
Rib cross sectional area, A_r (mm ²)	2.88
Ultimate tensile strength, T_u (kN/m)	18
Elements to be tested, N_s	5
Elements to be tested in one meter of width, N_m	48
Secant stiffness at 2.0% of strain, J_{sec} (kN/m)	796
Percentage of open area, f (%)	78

The principles of physical modelling with model geogrids [5] to quantify the effect on the parameters in the prototype geogrids, identified that the elongation at ultimate tensile strength and percentage of open area is unchanged between the model geogrid and prototype geogrid. Furthermore, for 1-g conditions the rib cross sectional area of the geogrid prototype has a ratio of $1/N$ to the model geogrid and the secant stiffness at 2.0% of strain and ultimate tensile strength of the prototype geogrid has a ratio of $1/N^2$ to the model geogrid. The ultimate tensile strength and secant stiffness at 2.0% of strain of the prototype PLA geogrid showed in this study values within the range of values of commercial geogrids. However, the elongation at ultimate tensile strength (2.8%) is very low compared to commercial geogrids.

4. Conclusions

This study presented the design and tensile testing of 1:2 model geogrids made of PLA and produced by the FDM process. A practical method to derive the uniaxial tensile properties of geogrids using longitudinal rib specimens was proposed, which proven to be an accurate technique to predict the secant stiffness. In general, the results encourage the development of 3D printed PLA geogrids for civil and geotechnical

engineering applications, in line with the recent emphasis on the sustainable economy. The following findings were made:

1. After applying the modelling physic techniques the PLA prototype geogrid show relatively good results of tensile strength about 18 kN/m, which was found to be comparable to that of fossil oil-derived polymer strip and geogrid;
2. lower elongation at failure (about 2.8%) than that of fossil oil-derived polymer geogrid, which would not affect geogrid's performance in geomaterial stabilisation;
3. printing process appears stable and replicable, and the influence of degradation of material tensile properties over time still need to be studied.

Acknowledgements

The scholarship BID/UBI - Santander Universidades/2018 is acknowledged. The authors thank Fabric Laboratory at Department of Textile Science and Technology for the assistance during the tensile testing.

References

- [1] NP EN ISO 10318-1:2016. Geossintéticos; Parte 1: Termos e definições (ISO 10318-1:2015). Instituto Português da Qualidade, 2016.
- [2] Vertematti JC. Brazilian manual of geosynthetics. Brazilian Association of Nonwoven and Technical Fabrics Industries; São Paulo, Brazil, 2004.
- [3] Walsh AT. Multi-axial grid or mesh structures with high aspect ratio ribs. United States patent. US 11,149,386. 31th January, 2017. Available from: <https://patft.uspto.gov/netahtml/PTO/>
- [4] Cislaghi A, Sala P, Borgonovo G, Gandolfi C, Bischetti GB. Towards more sustainable materials for geo-environmental engineering: The case of geogrids. Sustainability. 2021;13(5):2585. <https://doi.org/10.3390/su13052585>
- [5] Viswanadham BVS, König D. Studies on scaling and instrumentation of a geogrid. Geotextiles and Geomembranes. 2004;22(5):307–328. [https://doi.org/10.1016/s0266-1144\(03\)00045-1](https://doi.org/10.1016/s0266-1144(03)00045-1)
- [6] Stathas D, Wang JP, Ling HI. Model geogrids and 3D printing. Geotextiles and Geomembranes. 2017;45(6):688–696. <https://doi.org/10.1016/j.geotexmem.2017.07>
- [7] Wang S, Ma Y, Deng Z, Zhang S, Cai J. Effects of fused deposition modeling process parameters on tensile, dynamic mechanical properties

of 3D printed polylactic acid materials. *Polymer Testing*. 2020;86:106483.
<https://doi.org/10.1016/j.polymertesting.2020.106483>

- [8] Oliveira G, Falorca I. Stress-strain relationship in homogeneous and two-layered triaxial test specimens. *KnE Engineering*. 2020;5(5):88-99.
<https://doi.org/10.18502/keg.v5i5.6923>
- [9] NP EN ISO 10319:2016. Geossintéticos: Ensaio de tração em tiras largas (ISO 10319:2015). Instituto Português da Qualidade, 2016.